PHYSICAL REVIEW D **91,** 013004 (2015)

Nonzero θ_{13} and leptogenesis in a type-I seesaw model with A_4 symmetry

Biswajit Karmakar* and Arunansu Sil†

Indian Institute of Technology Guwahati, 781039 Assam, India

(Received 5 August 2014; published 14 January 2015)

In light of the recent discovery of nonzero θ_{13}, we have analyzed the Altarelli-Feruglio A_4 flavor symmetry model extended with additional flavon. The inclusion of the new field leads to the deviation from the exact tri-bimaximal neutrino mixing pattern in the context of a type-I seesaw by producing a nonzero θ_{13} consistent with the recent experimental results at the leading order. A sum rule for light neutrino masses is also obtained in this context. The setup constrains the two Majorana phases involved in the lepton mixing matrix in terms of A_4 parameter space. We have shown that a nonzero lepton asymmetry can be generated while next-to-leading order contributions to the neutrino Yukawa couplings are considered. The two Majorana phases play a crucial role in CP-asymmetry parameter and the involvement of θ_{13} in it, is exercised.

DOI: 10.1103/PhysRevD.91.013004 PACS numbers: 14.60.Pq, 14.60.St, 11.30.Hv, 12.60.-i

I. INTRODUCTION

The evidence of nonvanishing value of the mixing angle θ_{13} from several experiments (Double Chooz [1], Daya Bay [2], RENO [3], T2K [4]) receives particular attention in these days since the precise determination of neutrino mixing would be crucial for better understanding the issues related to the flavor. In this context it is important to study the neutrino mass matrix, m_ν, which can be structured from discrete flavor symmetry. The neutrino mass matrix m_ν, in general, can be diagonalized by the $U_{\rm PMNS}$ matrix (in the basis where charged leptons are diagonal) as

$$m_\nu = U^*_{\rm PMNS}\,\mathrm{diag}(m_1, m_2, m_3)\,U^\dagger_{\rm PMNS}, \tag{1.1}$$

where m_1, m_2, m_3 are the real mass eigenvalues. The standard parametrization [5] of the $U_{\rm PMNS}$ matrix is given by

$$U_{\rm PMNS} = \begin{bmatrix} c_{12}c_{13} & s_{12}c_{13} & s_{13}e^{-i\delta} \\ -s_{12}c_{23} - c_{12}s_{13}s_{23}e^{i\delta} & c_{12}c_{23} - s_{12}s_{13}s_{23}e^{i\delta} & c_{13}s_{23} \\ s_{12}s_{23} - c_{12}s_{13}c_{23}e^{i\delta} & -c_{12}s_{23} - s_{12}s_{13}c_{23}e^{i\delta} & c_{13}c_{23} \end{bmatrix} \begin{bmatrix} 1 & 0 & 0 \\ 0 & e^{i\alpha_{21}/2} & 0 \\ 0 & 0 & e^{i\alpha_{31}/2} \end{bmatrix}, \tag{1.2}$$

where $c_{ij} = \cos\theta_{ij}$, $s_{ij} = \sin\theta_{ij}$, δ is the CP-violating Dirac phase while α_{21} and α_{31} are the two CP-violating Majorana phases. Though the neutrino mixing angles θ_{12}, θ_{23} and the two mass-squared differences have been well measured at several neutrino oscillation experiments [6], only an upper bound was present (consistent with zero) for the other mixing angle θ_{13} until 2011 [7]. Then the recent results from Double Chooz [1], Daya Bay [2], RENO [3], and T2K [4] suggest that in fact θ_{13} is nonzero and of sizable magnitude. From the updated global analysis [8] involving all the data from neutrino experiments, we have 1σ and 3σ ranges of mixing angles and the mass-squared differences as mentioned (NH and IH stand for the normal and inverted mass hierarchies respectively) in Table I. Majorana phases are not appearing in neutrino oscillation probability and therefore cannot be constrained from neutrino oscillation data directly [9]. As of now, any specific constraint on the Dirac CP-violating phase δ is still missing and so it is ranged between 0 to 2π [8].

This clearly indicates a completely different pattern of mixing in the lepton sector compared to the quark sector. Efforts therefore have been exercised for a long time in realizing the neutrino mixing pattern and among them patterns based on discrete flavor groups attract particular attention. A case of special mention is where $\sin^2\theta_{12} = 1/3$, $\sin^2\theta_{23} = 1/2$ along with $\sin\theta_{13} = 0$ resulted, called the tri-bimaximal (TBM) mixing pattern [10]. Note that all these mixing angles inclusive of vanishing θ_{13} were in the right ballpark of experimental findings before 2011. Many discrete groups have been employed [11] in realizing the TBM mixing pattern, and A_4 turned out to be a special one which can reproduce this pattern in a most economic way [12–14]. A_4 is a discrete group of even permutations of four objects. It has three inequivalent one-dimensional representations $(1, 1', 1'')$ and a three-dimensional representation

*k.biswajit@iitg.ernet.in
†asil@iitg.ernet.in

TABLE I. Summary of neutrino oscillation parameters for normal and inverted neutrino mass hierarchy from the analysis of [8].

Oscillation parameters	1σ range	3σ range
Δm^2_{21}	7.42–7.79 [10^{-5} eV^2]	7.11–8.18
$\lvert\Delta m^2_{31}\rvert$	2.41–2.53 [10^{-3} eV^2] (NH)	2.30–2.65
	2.32–2.43 [10^{-3}eV^2] (IH)	2.20–2.54
$\sin^2\theta_{12}$	0.307–0.339	0.278–0.375
$\sin^2\theta_{23}$	0.439–0.599 (NH)	0.392–0.643
	0.530–0.598 (IH)	0.403–0.640
$\sin^2\theta_{13}$	0.0214–0.0254 (NH)	0.0177–0.0294
	0.0221–0.0259 (IH)	0.0183–0.0297

(3). In this paper, we mostly concentrate on the Altarelli-Feruglio (AF) type of model [14] where the light neutrino masses are generated through a type-I seesaw mechanism. So the right-handed neutrinos (N^c) are introduced which transform as a triplet of A_4. Flavon fields transforming trivially and nontrivially under the A_4 are also introduced, whose vacuum expectation values (VEV) break the A_4 flavor symmetry at some high scale. The framework is supersymmetric and based on the standard model (SM) gauge interactions. As it was argued in [14], the introduction of supersymmetry was instrumental to provide the correct vacuum alignment. Then the type-I seesaw leads to the TBM mixing in the light neutrinos while the charged lepton mass matrix is found to be diagonal.

However, with the latest developments toward the nonzero value of θ_{13}, it is essential to modify the exact TBM pattern. Several attempts were made in this direction during past couple of years in the context of A_4-based flavor models [15–23]. It is to be noted from these analyses that inclusion of higher order terms only would not produce a sufficiently large θ_{13} as predicted by experiments. So a leading order deformation of the original A_4 model is required which we will study in this paper.

Another important phenomenon that cannot be realized in the context of the standard model is to explain the observed matter-antimatter asymmetry of the Universe. However, it is known that the standard weak interactions can lead to processes (mediated by sphalerons) which can convert the baryons and leptons. So a baryon asymmetry can be effectively generated from a lepton asymmetry. The mechanism for generating the lepton asymmetry is called leptogenesis [24]. The discussion of it is of particular importance here, while explaining the generation of light neutrino mass through a type-I seesaw mechanism. The inclusion of heavy right-handed (RH) neutrinos in the framework provides the opportunity to discuss also the leptogenesis scenario through the CP-violating decay of it in the early Universe. Although the ingredients (RH neutrinos) are present, it is known that the seesaw models predicting the exact TBM structure cannot generate the required lepton asymmetry [25], the reason being the term involved in the asymmetry related to the neutrino Yuwaka coupling matrix is proportional to the identity matrix and thus the lepton number asymmetry parameter vanishes. However it was shown in [25] that one can in principle consider higher dimensional operators in the neutrino Yukawa couplings of the model. The effect of this inclusion is to deviate the products of the Yukawa terms in lepton asymmetry parameter from unity and thereby generating nonzero lepton asymmetry.

In this paper, our aim is to produce nonzero θ_{13} as well as to realize leptogenesis in the same framework. We have extended the flavon sector of AF [14] by introducing an extra flavon, ξ' which transforms as $1'$ under A_4. A similar sort of extensions has been considered in [16,18]. However the analyses in those papers are mostly related to the deviation over the final form of m_ν obtained from the AF model, while here we consider modification of m_ν through the deviation from the RH neutrino mass matrix M_R. In [20,26], a perturbative deviation from tri-bimaximal mixing is considered through M_R, though leptogenesis was not considered in that framework. This provides the opportunity to analyze M_R in detail and the effect on the Majorana phases can also be studied. Inclusion of Z_3 symmetry in the model forbids several unwanted terms and thus helps in constructing specific structure of the coupling matrices. While the charged lepton mass matrix is found to be in the diagonal form, the RH neutrino mass matrix has an additional structure originated from the ξ'-related term. Due to this, the light neutrino diagonalizing matrix no longer remains in TBM form rather a deviation is resulted which leads to nonzero θ_{13}. In the RH neutrino mass matrix, three complex parameters a, b and d are present. We found that the low energy observables can be expressed in terms of two parameters $\lambda_1(=|d/a|)$, $\lambda_2(=|b/a|)$; the relative phase between b and a (ϕ_{ba}) and $|a|$. The relative phase between d and a is assumed to be zero for simplicity. We have studied the dependence of θ_{13} on λ_1. The allowed range of θ_{13} restricts the range of the parameter space of λ_1. Then following the analysis [27], we are able to constrain also the Majorana phases (α_{21}, α_{31}) involved in the $U_{\rm PMNS}$ and study their dependence on the parameter λ_2 (for this we have fixed λ_1 to its value that corresponds to the best-fit value of $\sin^2\theta_{13}$) for both normal and inverted hierarchy cases. In this scenario, we obtain a general sum rule involving the light neutrino masses $m_{i=1,2,3}$ and the Majorana phases, α_{21}, α_{31}. The effective mass parameter involved in the neutrinoless double beta decay is also estimated. We then investigate the generation of lepton asymmetry from the decay of RH neutrinos within "one flavor approximation" [27–30]. As previously stated, nonzero lepton asymmetry can be obtained once we include the next-to-leading order terms in the Yukawa sector. Note that this inclusion does not spoil the diagonal nature of charged lepton mass matrix. The explicit appearance of

TABLE II. Fields content and transformation properties under the symmetries imposed on the model. Here ω is the third root of unity.

	e^c	μ^c	τ^c	L_i	N_i^c	H_u	H_d	ϕ_S	ϕ_T	ξ	ξ'	ϕ_0^S	ϕ_0^T	ξ_0
A_4	1	$1''$	$1'$	3	3	1	1	3	3	1	$1'$	3	3	1
Z_3	ω	ω	ω	ω	ω^2	1	ω	ω^2	1	ω^2	ω^2	ω^2	1	ω^2
$U(1)_R$	1	1	1	1	1	0	0	0	0	0	0	2	2	2

these Majorana phases in the CP-asymmetry parameter, ϵ_i, provides the possibility of studying the dependence of ϵ_i on λ_2. The expression of ϵ_i also involves the θ_{13} mixing angle in our setup. Since θ_{13} depends on λ_1, we have also studied the variation of ϵ_i (or baryon asymmetry Y_B) against θ_{13} while λ_2 is fixed at a suitable value.

In Sec. II, we describe the structure of the model by specifying the fields involved and their transformation properties under the symmetries imposed. Then in Sec. III, we discuss the eigenvalues and phases involved in the RH neutrino sector. We also find the lepton mixing matrix and study the correlation between the mixing angles in terms of λ_1. Section IV is devoted to study the Majorana phases, light neutrino masses, effective mass parameter involved in neutrinoless double beta decay. Leptogenesis is analyzed in Sec. V and, following that, we have the conclusion in Sec. VI.

II. STRUCTURE OF THE MODEL

We consider here an extension of the original Altarelli-Feruglio (AF) model [14] (with right-handed neutrinos) for generating lepton masses and mixing by introducing one additional flavon ξ' which transforms as $1'$ under A_4. We will find this modification turns out to be instrumental to have nonzero θ_{13}. The particle content and the symmetries of the model are provided in Table II. The framework is supersymmetric and the gauge group is the same as that of the standard model. All the left-handed doublets $L_{i(=1,2,3)}$ transform as A_4 triplets, and the RH charged leptons e^c, μ^c, τ^c are A_4 singlets 1, $1''$, $1'$ respectively. In order to realize the type-I seesaw, three right-handed neutrinos (N_i^c) are considered which are triplets of A_4. The flavor symmetry A_4 is accompanied by a discrete Z_3 symmetry, which forbids several unwanted terms. The A_4 multiplication rules are mentioned in Appendix A. There are four flavons (ϕ_S, ϕ_T, ξ, ξ') in the model, which are SM gauge singlets. When the flavons (the scalar component of it) get vacuum expectation values (VEV), $\langle\phi_S\rangle = (v_S, v_S, v_S)$, $\langle\phi_T\rangle = (v_T, 0, 0)$, $\langle\xi\rangle = u$, $\langle\xi'\rangle = u'$, the $A_4 \times Z_3$ symmetry is broken and generates the flavor structure of the sector. The fields ϕ_0^S, ϕ_0^T and ξ_0 are the driving fields, carrying two units of $U(1)_R$ charges, introduced to realize the vacuum alignments of the flavon fields, ϕ_S, ϕ_T, ξ, ξ'. Supersymmetry helps in realizing this vacuum alignment by setting the F-term to be zero. A brief discussion on the vacuum alignment is provided in Appendix B. H_u and H_d are the two Higgs doublets present in the setup transforming as singlets under A_4 with the VEVs v_u and v_d respectively. With the above-mentioned field configuration, the effective superpotential for the charged lepton sector contains the following terms in the leading order (LO):

$$w_L = [y_e e^c (L\phi_T) + y_\mu \mu^c (L\phi_T)' + y_\tau \tau^c (L\phi_T)''] \left(\frac{H_d}{\Lambda}\right), \tag{2.1}$$

where Λ is the cutoff scale of the theory and y_e, y_μ, y_τ are the coupling constants. Terms in the first parentheses represent products of two triplets (here L and ϕ_T for example) under A_4, each of these terms contracts with A_4 singlets 1, $1''$ and $1'$ corresponding to e^c, μ^c and τ^c respectively. Finally it sets the charged lepton coupling matrix as the diagonal one in the leading order,

$$Y_L = \frac{v_T}{\Lambda} \begin{bmatrix} y_e & 0 & 0 \\ 0 & y_\mu & 0 \\ 0 & 0 & y_\tau \end{bmatrix}, \tag{2.2}$$

once the flavon VEVs as well as the Higgs VEVs are inserted. The relative hierarchies between the charged leptons can be generated if one introduces global Froggatt-Nielsen [$U(1)_{\rm FN}$] flavor symmetry, under which RH charged leptons have different charges in addition to a FN field [31,32].

In the absence of the ξ' field, the neutrino sector would have the superpotential of the form

$$w_\nu = y(N^c L) H_u + x_A \xi (N^c N^c) + x_B (N^c N^c \phi_S), \tag{2.3}$$

which yields the Dirac (m_D) and Majorana (M_R) neutrino mass matrices at the LO as given by

$$m_D = y v_u \begin{bmatrix} 1 & 0 & 0 \\ 0 & 0 & 1 \\ 0 & 1 & 0 \end{bmatrix} \equiv Y_{\nu 0} v_u;$$
$$M_R = \begin{bmatrix} a + 2b/3 & -b/3 & -b/3 \\ -b/3 & 2b/3 & a - b/3 \\ -b/3 & a - b/3 & 2b/3 \end{bmatrix}, \tag{2.4}$$

where $a = 2x_A u$, $b = 2x_B v_S$ and $Y_{\nu 0}$ can be taken as the LO neutrino Yukawa coupling matrix. Here y, x_A, and x_B

are respective coupling constants. It has been known [12–14] that this kind of structure produces the exact TBM mixing, predicting $\theta_{13}=0$. However in our setup, the inclusion of ξ' ensures the presence of another term in the superpotential w_ν, given by

$$x_N\xi'(N^cN^c), \tag{2.5}$$

at the LO, where x_N is another coupling constant. It introduces a modified Majorana mass matrix, compared to the one (M_R) in the TBM case, having the form

$$M_{Rd}=\begin{bmatrix} a+2b/3 & -b/3 & -b/3 \\ -b/3 & 2b/3 & a-b/3 \\ -b/3 & a-b/3 & 2b/3 \end{bmatrix}+\begin{bmatrix} 0 & 0 & d \\ 0 & d & 0 \\ d & 0 & 0 \end{bmatrix}, \tag{2.6}$$

where $d=2x_Nu'$. Since this additional term is also at the renormalizable level, we expect the term d to be of the order of a and b, in general. Inclusion of higher order terms in m_D would be very important in having leptogenesis as we will discuss in Sec. V.

In general we expect the VEVs of the flavon fields (v_S, v_T, u, u') are of the same order of magnitude $\sim v$ (say). Therefore, the magnitude of light neutrino m_ν becomes $\sim(yv_u)^2/v$, generated through a type-I seesaw mechanism. However, there could be operators like $(LH_u)(LH_u)$, which can also contribute to the light neutrino mass. In our model such terms appear only in combination with ϕ_S, ξ and ξ' in quadrature ($LH_uLH_u\frac{1}{\Lambda^3}[\phi_S^2,\phi_S\xi,\phi_S\xi',\xi\xi',\xi'^2]$), as LH_uLH_u is not an invariant under Z_3. Note that these terms contribute to the light neutrino mass of order $\frac{v_u^2}{v}\kappa^3$ where $\kappa=\frac{v}{\Lambda}\ll 1$. Hence they are relatively small compared to the neutrino mass generated from a type-I seesaw by order of κ^3 with $y\sim\mathcal{O}(1)$ or so and therefore can be neglected in the subsequent analysis.

There are next-to-leading order (NLO) corrections present in the model which are suppressed by $1/\Lambda^n$ with $n\geq 1$. For the charged lepton, the leading order (LO) contribution $f^c(L\phi_T)\frac{H_d}{\Lambda}$ ($f^c=e^c,\tau^c,\mu^c$), is already $1/\Lambda$ suppressed. So possible NLO contributions are $f^c(L(\phi_T\phi_T)_A)\frac{H_d}{\Lambda^2}$ and $f^c(L(\phi_T\phi_T)_S)\frac{H_d}{\Lambda^2}$, where the suffixes A and S stand for antisymmetric and symmetric triplet components from the product of two triplets in the first parenthesis under A_4. Now the first term essentially vanishes from the direction of VEVs of ϕ_T and the contribution coming from the second term is again diagonal, similar to the one obtained from the LO term. So a mere redefinition of y_e, y_μ, y_ν would keep the charged lepton matrix as a diagonal, even if NLO contributions are incorporated. This conclusion is in line with earlier observations [14,25].

We could as well include higher order terms involving $1/\Lambda$ (which are allowed by all the symmetries imposed) to the neutrino Yukawa coupling as $x_C(N^cL)_S\phi_TH_u/\Lambda+x_D(N^cL)_A\phi_TH_u/\Lambda$, with x_C and x_D as coupling constants. Therefore, at the next-to-leading order, the neutrino Yukawa coupling matrix can be rewritten as

$$\begin{aligned} Y_\nu &= Y_{\nu 0}+\delta Y_\nu \\ &= y\begin{bmatrix} 1 & 0 & 0 \\ 0 & 0 & 1 \\ 0 & 1 & 0 \end{bmatrix}+\frac{x_Cv_T}{\Lambda}\begin{bmatrix} 2 & 0 & 0 \\ 0 & 0 & -1 \\ 0 & -1 & 0 \end{bmatrix} \\ &\quad +\frac{x_Dv_T}{\Lambda}\begin{bmatrix} 0 & 0 & 0 \\ 0 & 0 & -1 \\ 0 & 1 & 0 \end{bmatrix}. \end{aligned} \tag{2.7}$$

This will not produce any significant effect on the light neutrino masses and mixing obtained through the type-I seesaw mechanism primarily with leading order m_D and M_{Rd}, as those terms are suppressed by the cutoff scale Λ compared to the LO contribution. However these will have an important role in leptogenesis, which we will discuss in Sec. V.

For RH Majorana neutrinos, the nonvanishing NLO corrections in the mass matrix arise from the following terms:

$$\begin{aligned} \delta M_{Rd} &= C_1(N^cN^c)_S\phi_T\xi/\Lambda+C_2(N^cN^c)_A\phi_T\xi'/\Lambda \\ &\quad +C_3(N^cN^c)(\phi_S\phi_T)/\Lambda+C_4(N^cN^c)''(\phi_S\phi_T)'/\Lambda \\ &\quad +C_5(N^cN^c)'(\phi_S\phi_T)''/\Lambda \\ &\quad +C_6(N^cN^c)_S(\phi_S\phi_T)_S/\Lambda \\ &\quad +C_7(N^cN^c)_S(\phi_S\phi_T)_A/\Lambda. \end{aligned} \tag{2.8}$$

Here $C_{i=1,\ldots,7}$ are the respective couplings and prefixes $'$ and $''$ correspond to the $1'$ and $1''$ singlets of A_4 produced from the multiplication of two triplets under A_4 within $(\cdots)$. Terms proportional to C_3 and C_4 can be absorbed in M_{Rd} and contributions from the remaining terms produce a deviation from M_{Rd} that can be written in a compact form as

$$\Delta M_{Rd}=\begin{bmatrix} 2X_D & X_B & -X_A \\ X_B & 2X_A & X_D \\ -X_A & X_D & X_B \end{bmatrix},$$

where $X_D=(3C_6v_s+C_7v_s+C_1u)\kappa$, $X_B=C_5v_s\kappa$ and $X_A=(2C_7v_s+C_2u_N)\kappa$. An almost similar type of conclusion was obtained in [27], apart from the fact that we have absorbed the term proportional to C_4 in the LO contribution of M_{Rd} and a new contribution coming from C_2 (through ξ') is included in the definition of X_A.

III. NEUTRINO MASSES AND MIXING

A light neutrino mass matrix is obtained through the type-I seesaw mechanism as $m_\nu = m_D^T M^{-1} m_D$, where M is the Majorana mass matrix for RH neutrinos. Note that the Majorana mass matrix M, with the form M_R as in Eq. (2.4) (i.e., without ξ' field), can be diagonalized through $U_{TB}^T M_R U_{TB} = \mathrm{diag}(M_{R1}e^{i\phi_1}, M_{R2}e^{i\phi_2}, M_{R3}e^{i\phi_3})$, where U_{TB} exhibits the TBM mixing pattern [10] and is described by

$$U_{TB} = \begin{bmatrix} \sqrt{\frac{2}{3}} & \frac{1}{\sqrt{3}} & 0 \\ -\frac{1}{\sqrt{6}} & \frac{1}{\sqrt{3}} & \frac{1}{\sqrt{2}} \\ -\frac{1}{\sqrt{6}} & \frac{1}{\sqrt{3}} & -\frac{1}{\sqrt{2}} \end{bmatrix}, \tag{3.1}$$

and $M_{R1,2,3}$ are given by $|b+a|$, $|a|$ and $|b-a|$ respectively. $\phi_{1,2,3}$ are the arguments of the eigenvalues respectively. It is found [20] that the light neutrino mass matrix m_ν $(= m_D^T M_R^{-1} m_D)$ in this case can also be diagonalized by a matrix U which is the same as U_{TB} except the second and third rows of it are interchanged (apart from the phases involved), so as to have $U^T m_\nu U = \mathrm{diag}(m_1, m_2, m_3)$. The light neutrino mass eigenvalues m_i are given by $m_i = (y v_u)^2/M_{Ri}$, and they can be made real and positive since the phase of y can be absorbed due to redefinition of phases in lepton doublets and the phases ϕ_i can be included in the diagonal phase matrix of U. As previously discussed, this structure of M_R is not useful in explaining the nonzero θ_{13}, as seen while comparing the above form of U and U_{PMNS}. Since the measured value of θ_{13} is not very small, it is difficult to reconcile θ_{13} just by deforming m_ν from its above form with the introduction of a small expansion parameter [33]. Rather we should have a deformation parameter at the same order of the existing elements in m_ν. In our framework, we have introduced the ξ' field for this purpose.

A. RH neutrinos

The new scalar singlet ξ' contributes to the heavy RH neutrino sector through the $x_N \xi'(N^c N^c)$ term and the Majorana neutrino mass matrix then takes the form of M_{Rd} as in Eq. (2.6). We note that after having a rotation by U_{TB}, the M_{Rd} takes the form as given by

$$U_{TB}^T M_{Rd} U_{TB} = \begin{bmatrix} a+b-\frac{d}{2} & 0 & -\frac{\sqrt{3}}{2}d \\ 0 & a+d & 0 \\ -\frac{\sqrt{3}}{2}d & 0 & -a+b+\frac{d}{2} \end{bmatrix}. \tag{3.2}$$

Therefore a further rotation by U_1 (another unitary matrix) takes the matrix M_{Rd} to a diagonal one, $\mathrm{diag}(M_1 e^{i\varphi_1}, M_2 e^{i\varphi_2}, M_3 e^{i\varphi_3}) = (U_{TB}U_1)^T M_{Rd} U_{TB} U_1$, where $M_{i=1,2,3}$ are given by

$$M_1 = |b + \sqrt{a^2+d^2-ad}| = |a||\lambda_2 e^{i\phi_{ba}} + \sqrt{1+\lambda_1^2 e^{2i\phi_{da}} - \lambda_1 e^{i\phi_{da}}}|, \tag{3.3}$$

$$M_2 = |a+d| = |a||1+\lambda_1 e^{i\phi_{da}}|, \tag{3.4}$$

$$M_3 = |b - \sqrt{a^2+d^2-ad}| = |a||\lambda_2 e^{i\phi_{ba}} - \sqrt{1+\lambda_1^2 e^{2i\phi_{da}} - \lambda_1 e^{i\phi_{da}}}|, \tag{3.5}$$

with $\lambda_1 = |d/a|$ and $\lambda_2 = |b/a|$. $\phi_{da} = \phi_d - \phi_a$ and $\phi_{ba} = \phi_b - \phi_a$ are the phase differences between (d,a) and (b,a) respectively. Phases associated with the above masses can be written as

$$\varphi_1 = \arg(b + \sqrt{a^2+d^2-ad}), \tag{3.6}$$

$$\varphi_2 = \arg(a+d), \tag{3.7}$$

$$\varphi_3 = \arg(b - \sqrt{a^2+d^2-ad}). \tag{3.8}$$

For simplicity, we will work with $\phi_{da} = 0$. Hence, the above set of eigenvalues and phases can be rewritten as

$$M_1 = |a||\lambda_2 e^{i\phi_{ba}} + \mathrm{K}| \qquad \varphi_1 = \arg(b + a\mathrm{K}), \tag{3.9}$$

$$M_2 = |a||1+\lambda_1| \qquad \varphi_2 = \arg(a+d), \tag{3.10}$$

$$M_3 = |a||\lambda_2 e^{i\phi_{ba}} - \mathrm{K}| \qquad \varphi_3 = \arg(b - a\mathrm{K}), \tag{3.11}$$

where $\mathrm{K} = \sqrt{1-\lambda_1+\lambda_1^2}$.

B. Light neutrino masses and mixing angles

The light neutrino masses obtained via a type-I seesaw mechanism through $m_\nu = m_D^T M_{Rd}^{-1} m_D$ are now given by $m_D^T U_R U_m^* [\mathrm{diag}(M_1, M_2, M_3)]^{-1} U_m^* U_R^T m_D$, where $U_R = U_{TB}U_1$ and $U_m = \mathrm{diag}(e^{i\varphi_1/2}, e^{i\varphi_2/2}, e^{i\varphi_3/2})$. The special form of m_D [see in Eq. (2.4)] suggests that U_R, with the second and third rows interchanged, will be the diagonalizing matrix of the light neutrino mass matrix m_ν apart from the diagonal phase matrix. Since the charged lepton mass matrix is already diagonal, the lepton mixing matrix is given by [20]

$$U_\nu = \frac{m_D^T}{y v_u} U_{TB} U_1^* \mathrm{diag}(e^{i\varphi_1/2}, e^{i\varphi_2/2}, e^{i\varphi_3/2}), \tag{3.12}$$

so that $m_\nu = U_\nu^* \mathrm{diag}(m_i) U_\nu^\dagger$. Note that the light neutrino masses $m_{1,2,3}$ (real and positive) are given by

$$m_i = \frac{(y v_u)^2}{M_i}, \tag{3.13}$$

where $M_{i=1,2,3}$ are taken from Eqs. (3.9)–(3.11). We can now remove one common phase by setting $\varphi_1 = 0$. Hence, the final form of unitary matrix that diagonalizes m_ν is given by

$$U_\nu = \frac{m_D^T}{y v_u} U_{TB} \begin{bmatrix} \cos\theta & 0 & \sin\theta e^{-i\psi} \\ 0 & 1 & 0 \\ -\sin\theta e^{i\psi} & 0 & \cos\theta \end{bmatrix} \mathrm{diag}(1, e^{i\varphi_2/2}, e^{i\varphi_3/2}), \tag{3.14}$$

$$= \begin{bmatrix} \sqrt{\frac{2}{3}}\cos\theta & 1/\sqrt{3} & \sqrt{\frac{2}{3}}\sin\theta e^{-i\psi} \\ -\frac{\cos\theta}{\sqrt{6}} + \frac{\sin\theta}{\sqrt{2}} e^{i\psi} & 1/\sqrt{3} & -\frac{\cos\theta}{\sqrt{2}} - \frac{\sin\theta}{\sqrt{6}} e^{-i\psi} \\ -\frac{\cos\theta}{\sqrt{6}} - \frac{\sin\theta}{\sqrt{2}} e^{i\psi} & 1/\sqrt{3} & \frac{\cos\theta}{\sqrt{2}} - \frac{\sin\theta}{\sqrt{6}} e^{-i\psi} \end{bmatrix} . \begin{bmatrix} 1 & 0 & 0 \\ 0 & e^{i\varphi_2/2} & 0 \\ 0 & 0 & e^{i\varphi_3/2} \end{bmatrix}, \tag{3.15}$$

where we have parametrized the extra U_1 matrix by θ and ψ and employed Eqs. (2.4) and (3.1). We identify the Majorana phases as

$$\varphi_2 = \alpha_{21} \quad \text{and} \quad \varphi_3 = \alpha_{31}. \tag{3.16}$$

In this type of model, using Eqs. (3.9)–(3.11) and Eq. (3.13) we find a general sum rule for light neutrino masses satisfying

$$\frac{1}{m_1} - \frac{2\mathrm{K} e^{i\alpha_{21}}}{m_2(1+\lambda_1)} = \frac{e^{i\alpha_{31}}}{m_3}. \tag{3.17}$$

Note that in the limit $\mathrm{K} \to 1$ (i.e., with $\lambda_1 = 0$), the sum rule is reduced to the one found in [27,34]. The Majorana phases α_{21} and α_{31} are therefore related to the light neutrino masses. They will play an important role in leptogenesis, which we discuss in Sec. V. The sum rule may carry an important consequence in neutrinoless double beta decay. A study with different sum rules in this direction can be found in [35].

The charged lepton mass matrix being diagonal, the above form of U_ν leads to [see Eq. (1.2)]

$$\sin\theta_{13} = \sqrt{\frac{2}{3}}\sin\theta, \qquad \delta = \psi; \tag{3.18}$$

$$\sin^2\theta_{12} = \frac{1}{3(1-\sin^2\theta_{13})} \qquad \text{and}$$

$$\sin^2\theta_{23} = \frac{1}{2} + \frac{1}{\sqrt{2}}\sin\theta_{13}\cos\delta, \tag{3.19}$$

up to the order $\sin^2\theta_{13}$. The study of these correlations in the presence of A_4 is available in the literature [20,22,36]. For rest of our analysis we will consider $\psi = 0$. The mixing angle θ is then given by

$$\tan 2\theta = \frac{\sqrt{3}\lambda_1}{(2-\lambda_1)}. \tag{3.20}$$

We have studied the variation of $\sin^2\theta_{13}$ against the parameter λ_1 in Fig. 1, where the 1σ and 3σ allowed regions for $\sin^2\theta_{13}$ obtained from [8] are also indicated in the same by red and blue horizontal shaded regions respectively for both NH and IH. We observe that for NH, the best fit [8] value of $\sin^2\theta_{13}$ ($= 0.0234$) corresponds to $\lambda_1 = 0.37$ and that one for IH ($\sin^2\theta_{13} = 0.024$) corresponds to $\lambda_1 = 0.38$. We also note that the 3σ range of $\sin^2\theta_{13}$ covers a narrow interval of λ_1 that can be approximately expressed as $0.33 \lesssim \lambda_1 \lesssim 0.41$ as seen from Fig. 1 for both NH and IH.

The other mixing angles θ_{12} and θ_{23} are also studied through the variation of $\sin^2\theta_{12}$ and $\sin^2\theta_{23}$ against λ_1, using Eq. (3.19) in Fig. 2. Note that once we restrict λ_1 to be in the above-mentioned range [indicated in Fig. 2 by vertical (blue) patches] so that $\sin^2\theta_{13}$ falls within the 3σ allowed range, it constrains the ranges of $\sin^2\theta_{12}$ and $\sin^2\theta_{23}$ in our setup. This result is mentioned in Table III as obtained from Fig. 2. The ranges are well within the 3σ allowed regions of $\sin^2\theta_{12}$ and $\sin^2\theta_{23}$ [8]. So we conclude that this particular range of λ_1 ($0.33 \lesssim \lambda_1 \lesssim 0.41$) is consistent in producing all three mixing angles successfully, and we will use this range of λ_1, while studying any other observables against λ_1 unless otherwise stated.

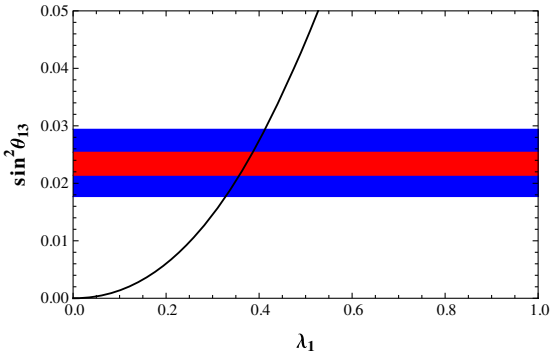

FIG. 1 (color online). $\sin^2\theta_{13}$ vs λ_1 (i.e., $|d/a|$) plot. The horizontal blue shaded region stands for the 3σ allowed range for $\sin^2\theta_{13}$ and the red shaded region inside represents the 1σ range for $\sin^2\theta_{13}$ obtained from [8].

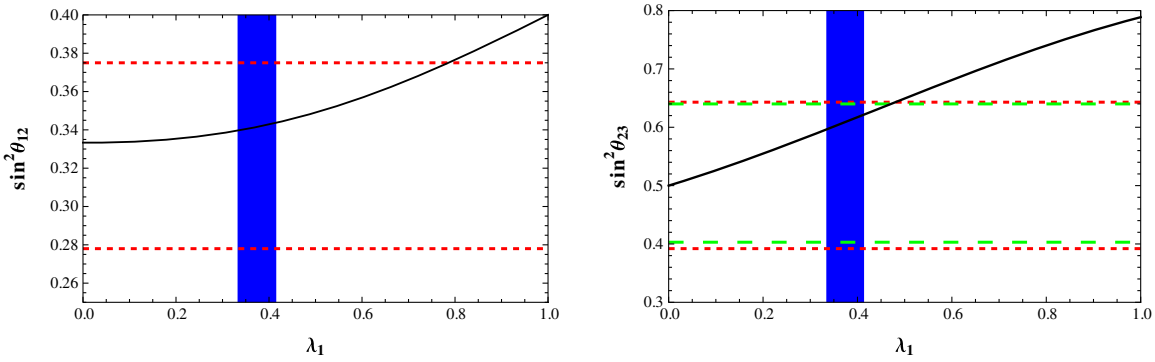

FIG. 2 (color online). λ_1 dependence of $\sin^2\theta_{12}$ and $\sin^2\theta_{23}$. The vertical blue patch indicates the restricted region of parameter space for λ_1 obtained from Fig. 1. The horizontal red dashed lines represent the 3σ allowed range for $\sin^2\theta_{12}$ in the left panel, while in the right panel the horizontal red dashed and green large-dashed lines represent 3σ allowed regions for $\sin^2\theta_{23}$ both NH and IH respectively as in [8].

IV. CONSTRAINTS ON PARAMETERS FROM NEUTRINO OSCILLATION DATA

Apart from λ_1, we have other parameters λ_2, $|a|$ and ϕ_{ba} (after setting $\phi_{da}=0$) in the right-handed neutrino sector. Note that λ_1, λ_2 and ϕ_{ba} can be constrained by neutrino oscillation data through the ratio of solar and atmospheric mass-squared differences ($\Delta m^2_\odot$ and $|\Delta m^2_A|$ respectively) defined by $r=\frac{\Delta m^2_\odot}{|\Delta m^2_A|}$ as exercised in [27,34]. These mass-squared differences are defined as $\Delta m^2_\odot=\Delta m^2_{21}=m_2^2-m_1^2$ and $|\Delta m^2_A|=|\Delta m^2_{31}|=m_3^2-m_1^2\approx|\Delta m^2_{32}|=m_3^2-m_2^2$. Following [8], the best fit values of $\Delta m^2_\odot=7.60\times10^{-5}$ eV^2 (for both NH and IH) and $|\Delta m^2_A|=2.48\times10^{-3}$ eV^2 [NH] (and $|\Delta m^2_A|=2.38\times10^{-3}$ eV^2 [IH]) will be used in our analysis. Using Eqs. (3.9)–(3.11), and (3.13) we obtain r in terms of parameters involved in our framework as given by

$$r=\frac{[\lambda_2^2+2\lambda_2\mathrm{K}\cos\phi_{ba}+\mathrm{K}^2-(1+\lambda_1)^2](\lambda_2^2-2\lambda_2\mathrm{K}\cos\phi_{ba}+\mathrm{K}^2)}{4(1+\lambda_1)^2\lambda_2\mathrm{K}|\cos\phi_{ba}|}. \tag{4.1}$$

We recall that ϕ_{ba} is the relative phase between parameters b and a. Note that with $\lambda_1=0$, K becomes unity and the expression for r gets back the form in [34]. Considering $\lambda_1<1$ (as required for θ_{13} being in the acceptable range, see Fig. 1) and as $\phi_{da}=0$, K becomes real and considered to be positive. Then as is evident from Eqs. (3.9)–(3.11) and (3.13), $\cos\phi_{ba}>0$ for NH and $\cos\phi_{ba}<0$ for IH. Using $r=0.03$ [8], we can use Eq. (4.1) now to study the correlation between λ_2 and $\cos\phi_{ba}$ as shown in Fig. 3. In doing so, we have set the value of λ_1 to be 0.37 (0.38) which corresponds to the best fit value of $\sin^2\theta_{13}$ for NH (IH) as stated before. Obviously the right panel of the plot corresponds to NH (as $\cos\phi_{ba}>0$) and the left panel is for IH (as $\cos\phi_{ba}<0$). We find that for NH, with $\lambda_1=0.37$, λ_2 is restricted to be in the range 0.71–1.2 and for IH, with $\lambda_1=0.38$, λ_2 falls within[1] the range 1.1–2.3. It will be further modified as we proceed after including the constraint on the sum of all the light neutrinos from the Planck data [37].

TABLE III. Allowed regions of $\sin^2\theta_{12}$ and $\sin^2\theta_{23}$ obtained from Fig. 2 for a restricted range of λ_1 (corresponding to Fig. 1) in our setup.

Range of λ_1 obtained from Fig. 1	$\sin^2\theta_{12}$	$\sin^2\theta_{23}$
$0.36\lesssim\lambda_1\lesssim0.39$	0.341–0.342	0.604–0.614
$0.33\lesssim\lambda_1\lesssim0.41$	0.339–0.343	0.595–0.620

The light neutrino mass m_1 in this framework can be expressed as

$$m_1^2=|\Delta m^2_A|r\frac{(1+\lambda_1)^2}{[\lambda_2^2+2\lambda_2\mathrm{K}\cos\phi_{ba}+\mathrm{K}^2-(1+\lambda_1)^2]}. \tag{4.2}$$

Now using the best fit value of $|\Delta m^2_A|=2.48\times10^{-3}$ eV^2 [NH] (2.38×10^{-3} eV^2 [IH]), $r=0.03$ and $\lambda_1=0.37$ (0.38), we can estimate m_1 from the above relation for NH (IH), shown in Fig. 4, as a function of λ_2. Similarly m_2 and m_3 are also plotted in Fig. 4. Note that in doing this, the correct sign of $\cos\phi_{ba}$ in Eq. (4.2) needs to be taken into

[1]Equation (4.1) describes a quadratic equation of $|\cos\phi_{ba}|$ once other parameters are fixed. The range of λ_2 between 0 and 0.71 is excluded to keep the discriminant positive for $\lambda_1=0.37$ (for NH).

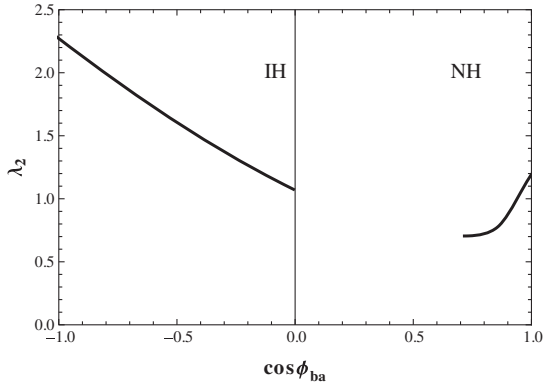

FIG. 3. Variation of λ_2 with $\cos\phi_{ba}$. Here we have fixed $\lambda_1 = 0.37$ for NH and $\lambda_1 = 0.38$ for IH.

account while NH and IH cases are considered. The lightest neutrino mass m_1 (m_3) falls in the range $0.008\ \text{eV} \lesssim m_1 \lesssim 0.02\ \text{eV}$ for NH ($0.02\ \text{eV} \lesssim m_3 \lesssim 0.12\ \text{eV}$ for IH). In this plot we have also shown the sum of the light neutrino masses, $\sum m_i$. From Fig. 4, we conclude that it lies in the range $0.07\ \text{eV} \lesssim \sum m_i \lesssim 0.1\ \text{eV}$ for NH and $0.13\ \text{eV} \lesssim \sum m_i \lesssim 0.28\ \text{eV}$ for IH. The Planck data along with external CMB and BAO results [37] provide an upper bound as $\sum m_i \lesssim 0.23\ \text{eV}$. Once this is considered, the range of $\sum m_i$ as obtained from our analysis for NH would not be affected. However in the case of IH, it further restricts the range of λ_2 ($1.3 \lesssim \lambda_2 \lesssim 2.3$, indicated by vertical dashed line) as observed from the shaded region of Fig. 4, right panel. So the model's prediction for a sum of all three light neutrino masses turns out to be

$$0.07\ \text{eV} \lesssim \sum_{i=1}^{3} m_i \lesssim 0.1\ \text{eV(NH)} \quad \text{and}$$
$$0.13\ \text{eV} \lesssim \sum_{i=1}^{3} m_i \lesssim 0.23\ \text{eV(IH)}. \tag{4.3}$$

In our analysis we can comment also on the relative magnitudes of heavy RH neutrinos. For NH we obtain $M_1 \simeq (1.1-1.5)M_2 \simeq (2.7-6.6)M_3$ and for IH we have $M_1 \simeq M_2 \simeq \frac{M_3}{1.2-2.3}$. So, in the present setup Majorana neutrinos are not strongly hierarchical.

Two Majorana phases α_{21} and α_{31} can be investigated in the setup in a similar way as done in [27]. Here in the model under consideration, we find Majorana phases α_{21} and α_{31} in terms of λ_1, λ_2 and ϕ_{ba} as given by

$$\tan\alpha_{21} = -\frac{\lambda_2 \sin\phi_{ba}}{\mathrm{K} + \lambda_2 \cos\phi_{ba}}, \tag{4.4}$$

$$\tan\alpha_{31} = \frac{2\mathrm{K}\lambda_2 \sin\phi_{ba}}{\lambda_2^2 - \mathrm{K}^2}. \tag{4.5}$$

Note that there exists a relative sign between $\sin\alpha_{21}$ and $\sin\alpha_{31}$ as observed from the neutrino mass sum rule in Eq. (3.17). For NH, $\cos\phi_{ba} > 0$ as discussed before and $\sin\phi_{ba} < 0$ is considered in order to produce the correct sign of baryon asymmetry [27]. Similarly, for IH we have $\cos\phi_{ba} < 0$ and $\sin\phi_{ba} < 0$. Taking all this into consideration, Eqs. (4.4) and (4.5) can successfully correlate Majorana phases (α_{21} and α_{31}) with parameters λ_1 and λ_2. We have plotted variation of α_{21} and α_{31} with λ_2 for both NH and IH in Figs. 5 and 6 respectively. As before we have fixed $\lambda_1 = 0.37$ for NH ($\lambda_1 = 0.38$ for IH). This study of Majorana phases will be particularly useful when we will study the dependence of CP-violating parameter ϵ_i in our model on λ_2. The effective neutrino mass parameter, $|\langle m\rangle|$, is an important quantity which controls the neutrinoless double beta decay. In our model, the effective neutrino mass parameter is obtained as [5,38]

$$|\langle m\rangle| = \left|\frac{2}{3}m_1\cos^2\theta + \frac{1}{3}m_2 e^{i\alpha_{21}} + \frac{2}{3}m_3\sin^2\theta e^{i\alpha_{31}}\right|. \tag{4.6}$$

Since the dependence of m_i and $\alpha_{21,31}$ on λ_2 (for fixed λ_1) is known (from Figs. 4–6), we plot $|\langle m\rangle|$ as a function of λ_2 with $\lambda_1 = 0.37$ for NH and $\lambda_1 = 0.38$ for IH in Fig. 7. We found the range for the $|\langle m\rangle|$ as $0.01\,\text{eV} < |\langle m\rangle| < 0.02\,\text{eV}$

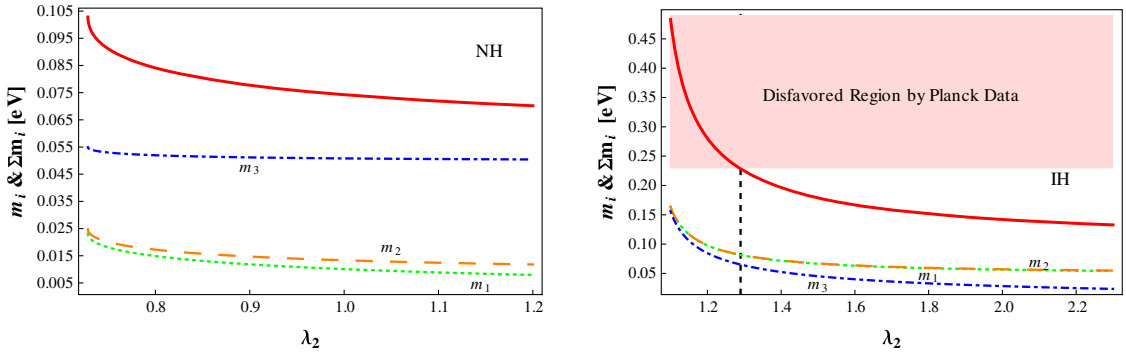

FIG. 4 (color online). Light neutrino masses m_i's and their sum, $\sum m_i$, as a function of λ_2 for NH ($\lambda_1 = 0.37$) and IH ($\lambda_1 = 0.38$). Here in the right panel the shaded region indicates the disfavored values of $\sum m_i$. This makes allowed range for λ_2 more restricted for IH, indicated by the vertical black dashed line.

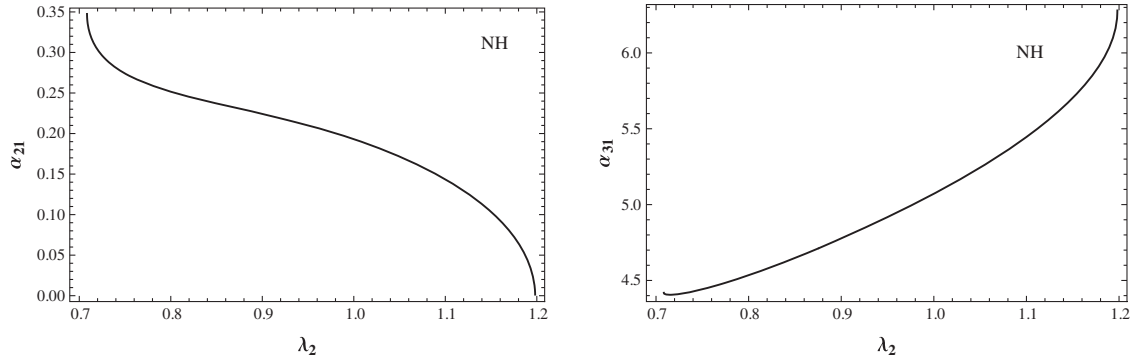

FIG. 5. Variation of Majorana phases (α_{21}: left panel; α_{31}: right panel) with λ_2 for NH.

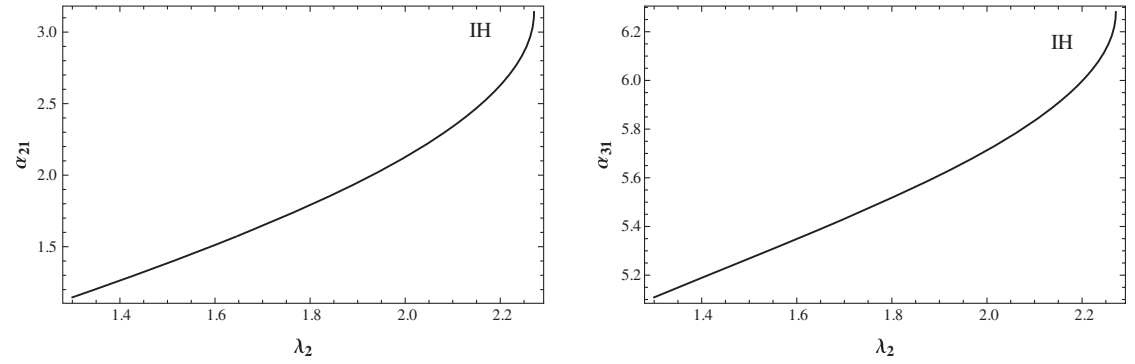

FIG. 6. Variation of Majorana phases (α_{21}: left panel; α_{31}: right panel) with λ_2 for IH.

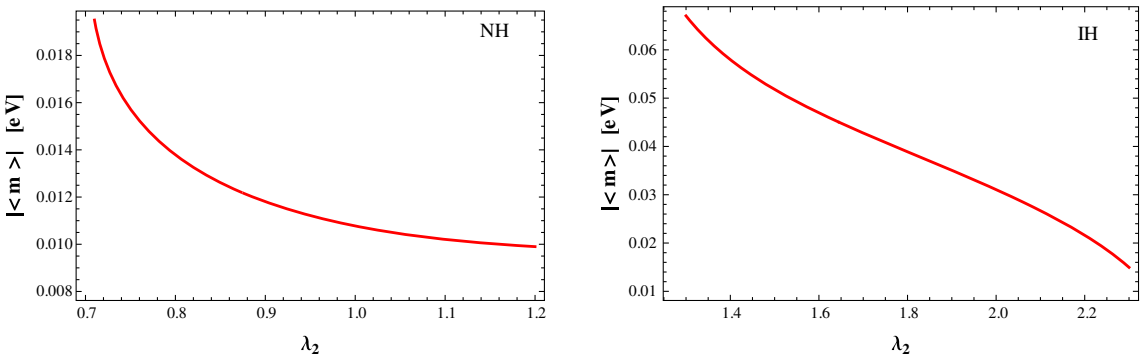

FIG. 7 (color online). Variation of $|\langle m\rangle|$ with λ_2 for NH (left panel) and IH (right panel) respectively.

for NH and $0.015\ \text{eV} < |\langle m\rangle| < 0.067\ \text{eV}$ for IH. The current upper limit on $|\langle m\rangle|$ however varies between 0.177 eV and 0.339 eV taking into account the different choices of nuclear matrix elements [39].

V. LEPTOGENESIS

The presence of seesaw realization of light neutrino mass in the model under consideration gives the opportunity to study leptogenesis as the heavy RH neutrinos are already present in the model. It allows the generation of lepton asymmetry through the out-of-equilibrium decay of heavy RH neutrinos in the early Universe. This lepton asymmetry can be converted into baryon asymmetry of the Universe with the help of sphaleron process. With the consideration that the generation of lepton asymmetry happens at a temperature of the Universe $T \sim M_i \gtrsim (1 + \tan^2\beta)10^{12}$ GeV (where $\tan\beta = v_u/v_d$), it does not distinguish between flavors, the so-called one flavor approximation regime [27–30] is achieved. The CP-asymmetry generated by the out-of-equilibrium decay of each RH neutrinos (and sneutrinos) is given by [40–46]

$$\epsilon_i = \frac{1}{8\pi}\sum_{j\neq i}\frac{\mathrm{Im}[((\hat{Y}_\nu\hat{Y}_\nu^\dagger)_{ji})^2]}{(\hat{Y}_\nu\hat{Y}_\nu^\dagger)_{ii}} f\left(\frac{m_i}{m_j}\right), \tag{5.1}$$

where $\hat{Y}_\nu$ is the effective Yukawa coupling matrix for neutrinos in the basis where RH neutrino mass matrix M_{Rd} is diagonal.[2] In the present setup, $\hat{Y}_\nu = \mathrm{diag}(1, e^{-i\alpha_{21}/2}, e^{-i\alpha_{31}/2}) U_R^T Y_\nu$, where $U_R = U_{TB} U_1$. The loop factor $f(x)$ in the above expression (the model being supersymmetric) is defined as follows [46]:

$$f(x) \equiv -x\left[\frac{2}{x^2-1} + \ln\left(1+\frac{1}{x^2}\right)\right], \tag{5.2}$$

with $x = m_i/m_j$. The total lepton asymmetry receives a contribution from the decay of all three RH neutrinos (and sneutrinos).

It has been observed that at LO (i.e., when $Y_\nu = Y_{\nu 0}$), the product of the effective Yukawa coupling matrices $\hat{Y}_{\nu 0}\hat{Y}_{\nu 0}^\dagger$ is proportional to a unit matrix, hence lepton asymmetry parameter ϵ_i vanishes [25]. However considering NLO corrections to the Yukawa, we have obtained Eq. (2.7). Therefore using Eq. (2.7), $\hat{Y}_\nu \hat{Y}_\nu^\dagger$ becomes

$$\begin{aligned}\hat{Y}_\nu \hat{Y}_\nu^\dagger = y^2 \mathbf{I} &+ \begin{bmatrix} \cos 2\theta & \sqrt{2} e^{\frac{i\alpha_{21}}{2}} \cos\theta & e^{\frac{i\alpha_{31}}{2}} \sin 2\theta \\ \sqrt{2} e^{-\frac{i\alpha_{21}}{2}} \cos\theta & 0 & \sqrt{2} e^{\frac{i(\alpha_{31}-\alpha_{21})}{2}} \sin\theta \\ e^{\frac{-i\alpha_{31}}{2}} \sin 2\theta & \sqrt{2} e^{\frac{-i(\alpha_{31}-\alpha_{21})}{2}} \sin\theta & -\cos 2\theta \end{bmatrix} (2\mathrm{Re}(x_C)\kappa y) \\ &+ \begin{bmatrix} -\frac{\sin 2\theta}{\sqrt{3}} & \sqrt{\frac{2}{3}} e^{\frac{i\alpha_{21}}{2}} \sin\theta & \frac{1}{\sqrt{3}} e^{\frac{i\alpha_{31}}{2}} \cos 2\theta \\ \sqrt{\frac{2}{3}} e^{-\frac{i\alpha_{21}}{2}} \sin\theta & 0 & -\sqrt{\frac{2}{3}} e^{\frac{i(\alpha_{31}-\alpha_{21})}{2}} \cos\theta \\ \frac{1}{\sqrt{3}} e^{\frac{-i\alpha_{31}}{2}} \cos 2\theta & -\sqrt{\frac{2}{3}} e^{\frac{-i(\alpha_{31}-\alpha_{21})}{2}} \cos\theta & \frac{1}{\sqrt{3}} \sin 2\theta \end{bmatrix} (2\mathrm{Re}(x_D)\kappa y). \end{aligned} \tag{5.3}$$

Note that having the origin related to a NLO correction term, κ in general is expected to be small, $\kappa = v_T/\Lambda \ll 1$. Hence the expression of Eq. (5.3) is kept up to first order in κ. Finally in our framework the CP-asymmetry parameters corresponding to all three RH neutrinos, $\epsilon_{1,2,3}$ take the form as

$$\begin{aligned}\epsilon_1 = \frac{-\kappa^2}{2\pi}\Bigg[&\sin\alpha_{21}\left(2\mathrm{Re}(x_C)^2\cos^2\theta + \frac{2\mathrm{Re}(x_D)^2}{3}\sin^2\theta + \frac{2\mathrm{Re}(x_C)\mathrm{Re}(x_D)}{\sqrt{3}}\sin 2\theta\right) f\left(\frac{m_1}{m_2}\right) \\ &+ \sin\alpha_{31}\left(\mathrm{Re}(x_C)^2\sin^2 2\theta + \frac{\mathrm{Re}(x_D)^2}{3}\cos^2 2\theta + \frac{\mathrm{Re}(x_C)\mathrm{Re}(x_D)}{\sqrt{3}}\sin 4\theta\right) f\left(\frac{m_1}{m_3}\right)\Bigg],\end{aligned} \tag{5.4}$$

$$\begin{aligned}\epsilon_2 = \frac{\kappa^2}{2\pi}\Bigg[&\sin\alpha_{21}\left(2\mathrm{Re}(x_C)^2\cos^2\theta + \frac{2\mathrm{Re}(x_D)^2}{3}\sin^2\theta + \frac{2\mathrm{Re}(x_C)\mathrm{Re}(x_D)}{\sqrt{3}}\sin 2\theta\right) f\left(\frac{m_2}{m_1}\right) \\ &- \sin(\alpha_{31}-\alpha_{21})\left(2\mathrm{Re}(x_C)^2\sin^2\theta + \frac{2\mathrm{Re}(x_D)^2}{3}\cos^2\theta - \frac{2\mathrm{Re}(x_C)\mathrm{Re}(x_D)}{\sqrt{3}}\sin 2\theta\right) f\left(\frac{m_2}{m_3}\right)\Bigg],\end{aligned} \tag{5.5}$$

$$\begin{aligned}\epsilon_3 = \frac{\kappa^2}{2\pi}\Bigg[&\sin\alpha_{31}\left(\mathrm{Re}(x_C)^2\sin^2 2\theta + \frac{\mathrm{Re}(x_D)^2}{3}\cos^2 2\theta + \frac{\mathrm{Re}(x_C)\mathrm{Re}(x_D)}{\sqrt{3}}\sin 4\theta\right) f\left(\frac{m_3}{m_1}\right) \\ &+ \sin(\alpha_{31}-\alpha_{21})\left(2\mathrm{Re}(x_C)^2\sin^2\theta + \frac{2\mathrm{Re}(x_D)^2}{3}\cos^2\theta - \frac{2\mathrm{Re}(x_C)\mathrm{Re}(x_D)}{\sqrt{3}}\sin 2\theta\right) f\left(\frac{m_3}{m_2}\right)\Bigg].\end{aligned} \tag{5.6}$$

Lepton asymmetry in this scenario therefore depends on light neutrino masses m_i (through loop factor), Majorana phases $\alpha_{21,31}$, couplings $\mathrm{Re}(x_{C,D})$, κ (coming from the NLO correction terms in Yukawa) and interestingly on θ (and hence on λ_1). Recall that θ was originated from the deviation from the exact tri-bimaximal mixing and therefore leads to nonzero $\sin\theta_{13}$. We will come back to discuss it; before that let us discuss how this lepton asymmetry parameter is connected with observed baryon asymmetry of the Universe.

Lepton asymmetry can be linked to the baryon asymmetry [24,47–49] as

$$Y_B = -1.48 \times 10^{-3} \sum_i \epsilon_i \eta_{ii}. \tag{5.7}$$

[2]Here Eq. (3.13) is used to express the loop factor f in terms of the ratio of light neutrino masses.

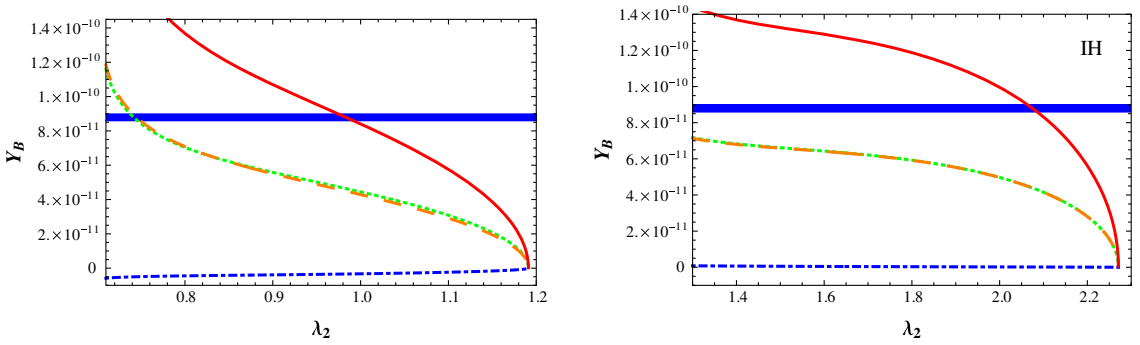

FIG. 8 (color online). Baryon asymmetry of the Universe as a function of λ_2 for NH (with $\lambda_1 = 0.37$, left panel) and IH (with $\lambda_1 = 0.38$, right panel). Here, the red continuous line, orange large dashed line, green dotted line and blue dot-dashed line stand for total Y_B, $Y_{B1,2,3}$ respectively. The horizontal blue patch represents the allowed range for total baryon asymmetry. For NH we have taken $\mathrm{Re}(x_C) = \mathrm{Re}(x_D) = 0.2$ and for IH we have $\mathrm{Re}(x_C) = \mathrm{Re}(x_D) = 0.05$. For both cases we have fixed κ at 0.01.

Here η_{ii} stands for the efficiency factor [46]. We consider the efficiency factor to be given by

$$\frac{1}{\eta_{ii}} \approx \frac{3.3 \times 10^{-3}\ \mathrm{eV}}{\tilde{m}_i} + \left(\frac{\tilde{m}_i}{0.55 \times 10^{-3}\ \mathrm{eV}}\right)^{1.16}, \quad (5.8)$$

with $\tilde{m}_i$ as the washout mass parameter, $\tilde{m}_i = \frac{(\hat{Y}_\nu \hat{Y}_\nu^\dagger)_{ii} v_u^2}{M_i} \simeq m_i$ to the leading order. The above expression is valid for $M_i < 10^{14}$ GeV [50]. This upper bound on M_i is also consistent in keeping the lepton number violating decays within the experimental limit [50,51]. As we already have a lower bound on M_i from the one flavor approximation, it turns out that low values of $\tan\beta$ are favored for this scenario to work.[3] Interestingly in [52], the authors have shown that if the scale of supersymmetry breaking (m_s) in minimal supersymmetric standard model is sufficiently large (say $\sim$10 TeV or so) the low $\tan\beta$ region $\tan\beta \lesssim$ (3–5) is consistent with the results of LHC so far. Such large value of m_s on the other hand can in principle reduce the branching ratio for the lepton flavor violating processes. However the details of this conjecture is beyond the scope of the present study.

A. Leptogenesis with fixed λ_1 and varying λ_2

In this section we will study the range of the parameters involved in the Y_B expression so as to reproduce the correct amount of matter-antimatter asymmetry of the Universe. The observed value of Y_B is reported to be [53]

$$Y_B = (8.79 \pm 0.20) \times 10^{-11}. \quad (5.9)$$

As the efficiency factor (η_{ii}) is found to be $\sim\mathcal{O}(10^{-2})$, ϵ_i should be of order $\mathcal{O}(10^{-6})$ in order to reproduce the correct amount of baryon asymmetry of the Universe. As discussed earlier, we have kept λ_1 to be fixed at 0.37 for NH (0.38 for IH) which corresponds to the best fit value of $\sin^2\theta_{13}$ [8]. We further note that the expression of Y_B involves θ which in turn is related to θ_{13}. So once λ_1 is fixed it would correspond to a particular value of θ. The expansion parameter $\kappa = v_T/\Lambda$ is taken to be $\sim 10^{-2}$. The variation of $\alpha_{21,31}$ and m_i's with λ_2 (for $\lambda_1 = 0.37$, 0.38 for NH and IH respectively) are already studied. Using this information, we can study the dependence of Y_B on λ_2 for fixed values of $\mathrm{Re}(x_C)$ and $\mathrm{Re}(x_D)$. The first bracketed expression in Eqs. (5.4)–(5.6) therefore serves merely as constant factor.

In Fig. 8 (left panel), we have plotted total baryon asymmetry Y_B (red continuous line) along with individual $Y_{B1,2,3}$ (orange large dashed, green dotted and blue dot-dashed lines respectively) against λ_2 for $\mathrm{Re}(x_C) = \mathrm{Re}(x_D) = 0.2$ in the case of NH. Note that the range of λ_2 0.71–1.2 for NH and 1.3–2.3 for IH was already fixed (from Figs. 3 and 4) for $\lambda_1 = 0.37$ (for NH) and $\lambda_1 = 0.38$ (for IH) respectively. The relative sign between $\sin\alpha_{21}$ and $\sin\alpha_{31}$ is fixed from the sum rule, Eq. (3.17). Their dependence on λ_2 is depicted in Fig. 5. In producing these plots, we recall that $\cos\phi_{ba} > 0$ for NH and $\cos\phi_{ba} < 0$ for IH. Also $\sin\phi_{ba} < 0$ is considered to produce correct sign of Y_B. In ϵ_1, $f(m_1/m_2)$ is of positive sign and remains dominant over $|f(m_1/m_3)|$ throughout the range of λ_2 by orders of magnitude. So an overall negative sign for ϵ_1 results when combined with $\sin\alpha_{21} > 0$ and $\sin\alpha_{31} < 0$ for the range of λ_2 inferred from Fig. 8. A similar conclusion can be drawn for ϵ_2. In this case $f(m_2/m_1)$ is negative and its magnitude is sufficiently large compared to $|f(m_2/m_3)|$ so that differences between magnitude of $\sin\alpha_{21}$ and $\sin(\alpha_{31} - \alpha_{21})$ cannot produce any sizable effect between the two terms [one is the set of terms proportional to $\sin\alpha_{21}$ and another is the similar set proportional to $\sin(\alpha_{31} - \alpha_{21})$] involved. So ϵ_2 is effectively dominated by the first term and overall it gives a negative contribution. In ϵ_3, however both the terms involved contribute almost equally and overall ϵ_3 contributes with opposite sign (also seen in the Fig. 8 terms of Y_{B3} which is negative, left panel) compared to $\epsilon_{1,2}$. As shown in Fig. 8 (left panel), the contribution

[3] y is expected to be $\sim\mathcal{O}(10^{-1})$ in order to reproduce correct m_i for this range of M_i.

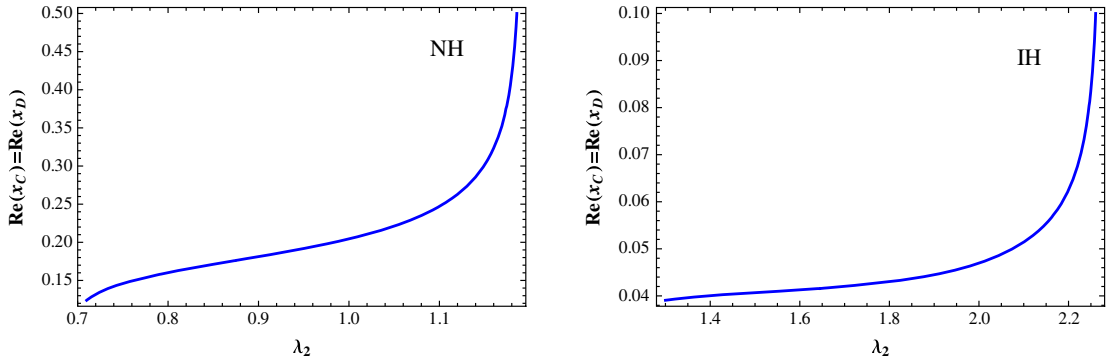

FIG. 9 (color online). Contour plot of $\mathrm{Re}(x_C)(=\mathrm{Re}(x_D))$ and λ_2, with Y_B fixed at its central value.

from Y_{B3} is suppressed (and of opposite sign). This is due to the fact that the corresponding washout is larger though in magnitude $|\epsilon_3| \lesssim |\epsilon_{1,2}|$. A horizontal patch in Fig. 8 is provided to indicate the allowed Y_B range [53]. It shows that for this specific choice of $\mathrm{Re}(x_{C,D}) = 0.2$, the correct amount of baryon asymmetry can be generated in our framework for $\lambda_2 \sim \mathcal{O}(1)$. Note that we can achieve this Y_B for not so large value of $\mathrm{Re}(x_{C,D})$ in comparison to the findings of [27]. To check the possible values of $\mathrm{Re}(x_C)$ and/or $\mathrm{Re}(x_D)$ we have drawn a contour plot in Fig. 9 (left panel) between $\mathrm{Re}(x_D)$ and λ_2, while $\mathrm{Re}(x_C) = \mathrm{Re}(x_D)$ is assumed as an example. The pattern of the Y_B plot is also different from what was obtained in [27]. This is due to the involvement of nonzero θ.

In Fig. 8 (right panel), we then plot Y_B, $Y_{B1,2,3}$ vs λ_2 in the case of IH with $\mathrm{Re}(x_C) = \mathrm{Re}(x_D) = 0.05$. As it was found in Sec. IV, λ_2 ranges between 1.3 and 2.3 and $\cos\phi_{ba} < 0$ and $\sin\phi_{ba} < 0$ in this case. The Majorana CP-violating phases α_{21} and α_{31} are obtained in Sec. IV as a function of λ_2 (see Fig. 6, with $\lambda_1 = 0.38$). Here m_1 and m_2 are much closer to each other leading to large enhancement in the magnitude of loop factors $f(m_1/m_2)$ and $f(m_2/m_1)$. Their magnitudes are even larger than their counterpart in NH. Variation of these loop factors with λ_2 shows that $f(m_1/m_2) \simeq -f(m_2/m_1) \gg f(m_3/m_{1,2})$ and $f(m_1/m_2) \simeq -f(m_2/m_1) \gg -f(m_{2,1}/m_3)$. Overall nonzero CP-violating phases α_{21} and α_{31} are required to have leptogenesis but it appears that the final asymmetry is dominated by the loop factors. Though Y_{B1} and Y_{B2} face a relatively large washout effect, still they generate a sizable contribution and Y_{B3} gives a subdominant contribution as shown in Fig. 8. Here also we have plotted a contour between $\mathrm{Re}(x_D)$ and λ_2, assuming $\mathrm{Re}(x_C) = \mathrm{Re}(x_D)$ with Y_B fixed at its central value, as shown in Fig. 9 (right panel). We find that in this case, smaller values of $\mathrm{Re}(x_C) = \mathrm{Re}(x_D)$ are favored compared to the ones in the NH case.

Since the RH Majorana neutrino masses (in IH case particularly) are close to each other, we need to check the possibility of satisfying condition for resonant leptogenesis [54]. In our model, the quantity related to the mass degeneracy has been computed and found to be

$$\frac{M_2}{M_1} - 1 \approx (10^{-2} - 10^{-3}), \tag{5.10}$$

after scanning over the full range of λ_2 ($1.3 \lesssim \lambda_2 \lesssim 2.3$). We find that the resonance condition,

$$\left|\frac{M_2}{M_1} - 1\right| \sim \left|\frac{(\hat{Y}_\nu \hat{Y}_\nu^\dagger)_{12}}{16\pi}\right|,$$

is not satisfied in our model. This is because the term in the right-hand side of the resonance condition turns out to be of order $5 \times 10^{-2} \kappa y [\mathrm{Re}(x_C)\cos\theta + \mathrm{Re}(x_D)\sin\theta]$. As $\kappa \sim 10^{-2}$, $y \sim 10^{-1}$ and θ is expected to produce correct θ_{13},

$$\frac{(\hat{Y}_\nu \hat{Y}_\nu^\dagger)_{12}}{16\pi} \sim 10^{-5} - 10^{-6}.$$

Hence, in the present model, the resonant condition is not satisfied.

B. Leptogenesis with fixed λ_2 and varying λ_1

In this case we have taken a different approach by keeping λ_2 fixed at a certain value, $\lambda_2 = 1$ for NH and $\lambda_2 = 2.1$ for IH.[4] Then we can study the variation of Y_B with λ_1. The range of λ_1 ($0.33 \lesssim \lambda_1 \lesssim 0.41$) is of course restricted from Fig. 1 in Sec. III. By using Eq. (4.1) and taking $r = 0.03$, we can now investigate the variation of $\cos\phi_{ba}$ vs λ_1. This is shown in Fig. 10. We find that $\cos\phi_{ba}$ does not vary much with λ_1 in the specified range. Similar to the one discussed in Sec. IV, we can also set the Majorana phases

[4]From Fig. 3 and the Planck limit on $\sum m_i$, note that no such common value of λ_2 exists for which both NH and IH cases can be considered.

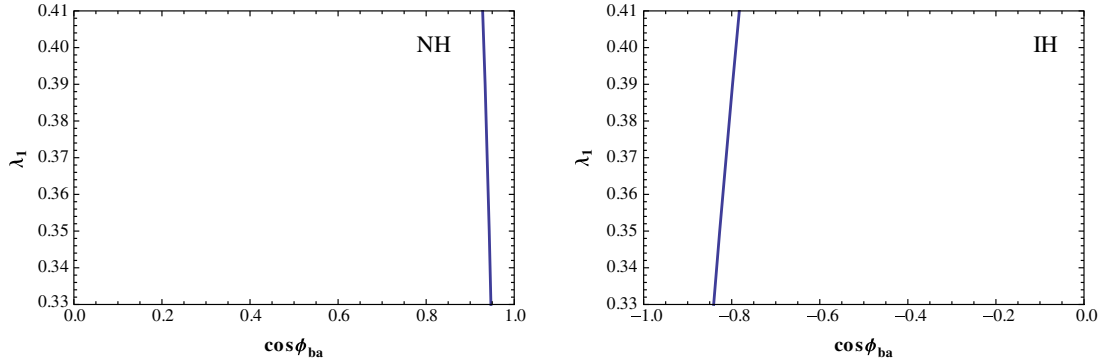

FIG. 10 (color online). $\cos\phi_{ba}$ vs λ_1 for $\lambda_2 = 1$ NH and $\lambda_2 = 2.1$ for IH.

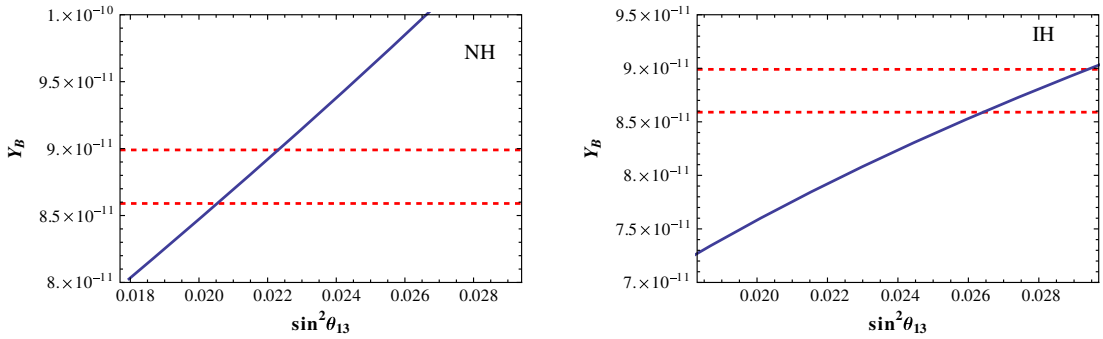

FIG. 11 (color online). Baryon asymmetry Y_B vs $\sin^2\theta_{13}$ for NH (left panel) and IH (right panel). Here the region between horizontal dashed lines represents observed value for Y_B from [53].

α_{21} and α_{31} as a function of λ_1 and finally we plot Y_B against $\sin^2\theta_{13}$ in Fig. 11 as $\sin^2\theta_{13}$'s dependence on λ_1 is known. Note that, here also we have used the values $\mathrm{Re}(x_{C,D}) = 0.2$ for NH and 0.05 for IH as before. The maximum value of the effective neutrino mass parameter turns out to be $|\langle m\rangle| \sim 0.01$ eV for NH (0.025 eV for IH).

VI. CONCLUSION

In this paper, we have studied the generation of nonzero θ_{13} in a A_4 symmetric framework. For this, we have extended the particle content of the AF model by adding one flavon, ξ'. In doing so, we consider the generation of light neutrino masses and mixing through the type-I seesaw mechanism. The addition of ξ' leads to a deformed structure for the right-handed neutrino mass matrix as compared to the one obtained in the case of a tri-bimaximal mixing pattern. The explicit structure of the right-handed neutrino mass matrix as well as the neutrino Yukawa matrices dictated by the flavor symmetry imposed $(A_4 \times Z_3)$ help in studying the mixing angles involved in the U_{PMNS} matrix. We find that our framework can reproduce all the mixing angles consistent with recent experimental findings for a restricted range of parameter space for λ_1 involved in the theory. We find a modified sum rule for this particular setup. Also the effective neutrino mass parameter $|\langle m\rangle|$ is studied. Since the structure of right-handed neutrino sector is known, it also opens up the possibility to study leptogenesis in this framework and particularly the involvement of Majorana phases in the setup can be utilized. Following [27], we then study the Majorana phases α_{21} and α_{31} involved in U_{PMNS} and their dependence on parameter λ_2, while keeping λ_1 fixed at a value that could reproduce the best fit value of $\sin^2\theta_{13}$. This is done while constraints on neutrino parameters like the ratio of Δm^2_{21} and Δm^2_{31} are considered in conjugation with the sum rule obtained. It is known that this sort of model will not generate lepton asymmetry due to the special form of neutrino Yukawa matrix involved. The same conclusion holds here also and we need to consider the next-to-leading order effect to the neutrino Yukawa sector in order to realize nonzero lepton asymmetry. We have calculated the next-to-leading order terms in our setup and their involvement in the expression for the CP-asymmetry parameter ϵ_i. Then we have shown that within one flavor approximation, our setup is able to generate a sufficient amount of lepton asymmetry through the decay of the right-handed neutrinos (and sneutrinos) without assigning large values to the parameters involved. In obtaining this result, we use the information obtained on the Majorana phases α_{21}, α_{31} as a function of

the parameters involved. As the baryon asymmetry can be linked with the generated lepton asymmetry finally we have studied the variation of baryon asymmetry parameter Y_B with λ_2. The effect of having nonzero θ_{13} is also studied.

It can also be noted that the framework restricts the RH neutrino masses in a narrow range between $(1+\tan^2\beta)10^{12}$ GeV and 10^{14} GeV as evident from the discussion below Eq. (5.8). This in turn can be used to estimate the scales involved in the theory. With our consideration that all the VEVs of the new scalars involved in the setup to be of similar order of magnitude, v, the RH neutrino masses are of order $M_i \sim 2xv$ as seen from Eqs. (3.9)–(3.11). With coupling constants $x \sim \mathcal{O}(1)$, it further tells that v is of order 10^{13} GeV with $\tan\beta \sim 3$. Therefore the new flavons [whose masses are proportional to v as seen from Eq. (B1)] are found to be as heavy as RH neutrinos, while the couplings involved are considered to be of order 1. So although the RH neutrinos have other interactions with the new scalars of the setup [from Eq. (2.3)], its decay mode is essentially dominated by the Yukawa interactions with the lepton and Higgs doublets only. This justifies our consideration of employing Eq. (5.1) which is the standard expression of leptogenesis for the decay of RH neutrinos through Yukawa interaction. Now, in order to produce a correct amount of lepton asymmetry, we require to have $\kappa = \frac{v}{\Lambda}$ to be of order 10^{-2}. This value is also consistent with the tau lepton mass as appeared in Eq. (2.1) with the coupling $y_\tau \sim \mathcal{O}(1)$. This sets the typical value of the cutoff scale Λ to be 10^{15} GeV. The close proximity of Λ with the grand unification scale turns out to be an intriguing feature of the model.

APPENDIX A: A_4 MULTIPLICATION RULES

A_4 is a discrete group of even permutation of four objects.[5] It has three inequivalent one-dimensional representations 1, $1'$, $1''$ and a irreducible three-dimensional representation 3. Products of the singlets and triplets are given by

$$\begin{aligned} 1 \otimes 1 &= 1, \\ 1' \otimes 1' &= 1'', \\ 1' \otimes 1'' &= 1, \\ 1'' \otimes 1'' &= 1', \quad \text{and} \\ 3 \otimes 3 &= 1 \otimes 1' \otimes 1'' \otimes 3_A \otimes 3_S, \end{aligned} \tag{A1}$$

where subscripts A and S stand for "asymmetric" and "symmetric" respectively. If we have two triplets (a_1, a_2, a_3) and (b_1, b_2, b_3); their products are given by

$$\begin{aligned} 1 &\sim a_1b_1 + a_2b_3 + a_3b_2, \\ 1' &\sim a_3b_3 + a_1b_2 + a_2b_1, \\ 1'' &\sim a_2b_2 + a_3b_1 + a_1b_3, \\ 3_S &\sim \begin{bmatrix} 2a_1b_1 - a_2b_3 - a_3b_2 \\ 2a_3b_3 - a_1b_2 - a_2b_1 \\ 2a_2b_2 - a_1b_3 - a_3b_1 \end{bmatrix}, \\ 3_A &\sim \begin{bmatrix} a_2b_3 - a_3b_2 \\ a_1b_2 - a_2b_1 \\ a_3b_1 - a_1b_3 \end{bmatrix}. \end{aligned} \tag{A2}$$

APPENDIX B: A_4 VACUUM ALIGNMENTS

In our model driving part of the LO superpotential, invariant under $A_4 \times Z_3$ with $R = 2$, can be written as

$$\begin{aligned} w_d = {} & M(\phi_0^T\phi_T) + g(\phi_0^T\phi_T\phi_T) \\ & + \phi_0^S(g_1\phi_S\phi_S + g_2\phi_S\xi + g_3\phi_S\xi') \\ & + \xi_0(g_4\phi_S\phi_S + g_5\xi\xi). \end{aligned} \tag{B1}$$

Equations which give vacuum structure of ϕ_T are given by

$$\begin{aligned} \frac{\partial w}{\partial \phi_{01}^T} &= M\phi_{T1} + \frac{2g}{3}(\phi_{T1}^2 - \phi_{T2}\phi_{T3}) = 0, \\ \frac{\partial w}{\partial \phi_{02}^T} &= M\phi_{T1} + \frac{2g}{3}(\phi_{T2}^2 - \phi_{T1}\phi_{T3}) = 0, \\ \frac{\partial w}{\partial \phi_{03}^T} &= M\phi_{T1} + \frac{2g}{3}(\phi_{T3}^2 - \phi_{T1}\phi_{T2}) = 0. \end{aligned} \tag{B2}$$

A solution of these equations can be given by $\langle\phi_T\rangle = (v_T, 0, 0)$ where $v_T = -\frac{3M}{2g}$. Again, equations responsible for vacuum alignments of ϕ_S, ξ and ξ' are

$$\begin{aligned} \frac{\partial w}{\partial \phi_{01}^S} &= \frac{2g_1}{3}(\phi_{S1}^2 - \phi_{S2}\phi_{S3}) + g_2\xi\phi_{S1} + g_3\xi'\phi_{S3} = 0, \\ \frac{\partial w}{\partial \phi_{02}^S} &= \frac{2g_1}{3}(\phi_{S2}^2 - \phi_{S1}\phi_{S3}) + g_2\xi\phi_{S3} + g_3\xi'\phi_{S2} = 0, \\ \frac{\partial w}{\partial \phi_{03}^S} &= \frac{2g_1}{3}(\phi_{S3}^2 - \phi_{S1}\phi_{S2}) + g_2\xi\phi_{S2} + g_3\xi'\phi_{S1} = 0, \\ \frac{\partial w}{\partial \xi_0} &= g_4(\phi_{S1}^2 + 2\phi_{S2}\phi_{S3}) + g_5\xi\xi = 0.. \end{aligned} \tag{B3}$$

From these equations we obtain $\langle\phi_S\rangle = (v_S, v_S, v_S)$, $\langle\xi\rangle = u$ and $\langle\xi'\rangle = u' \neq 0$ with $v_s^2 = \frac{-g_5u^2}{3g_4}$ and $u' = \frac{-g_2u}{g_3}$. Note that NLO correction terms with $1/\Lambda$ suppression involving ξ' in the superpotential w_d are absent and so the VEVs of the flavon fields remain unchanged.

[5]For a detailed discussion on A_4, see [32].

[1] Y. Abe *et al.* (DOUBLE-CHOOZ Collaboration), Phys. Rev. Lett. **108**, 131801 (2012).

[2] F. P. An *et al.* (DAYA-BAY Collaboration), Phys. Rev. Lett. **108**, 171803 (2012); Phys. Rev. D **90**, 071101 (2014).

[3] J. K. Ahn *et al.* (RENO Collaboration), Phys. Rev. Lett. **108**, 191802 (2012).

[4] K. Abe *et al.* (T2K Collaboration), Phys. Rev. Lett. **112**, 061802 (2014).

[5] J. Beringer *et al.* (Particle Data Group Collaboration), Phys. Rev. D **86**, 010001 (2012).

[6] S. Fukuda *et al.* (Super-Kamiokande Collaboration), Phys. Lett. B **539**, 179 (2002); Y. Ashie *et al.* (Super-Kamiokande Collaboration), Phys. Rev. D **71**, 112005 (2005); P. Adamson *et al.* (MINOS Collaboration), Phys. Rev. Lett. **106**, 181801 (2011); T. Araki *et al.* (KamLAND Collaboration), Phys. Rev. Lett. **94**, 081801 (2005).

[7] T. Schwetz, M. A. Tortola, and J. W. F. Valle, New J. Phys. **10**, 113011 (2008).

[8] D. V. Forero, M. Tortola, and J. W. F. Valle, Phys. Rev. D **90**, 093006 (2014).

[9] S. M. Bilenky, J. Hosek, and S. T. Petcov, Phys. Lett. B **94**, 495 (1980); P. Langacker, S. T. Petcov, G. Steigman, and S. Toshev, Nucl. Phys. **B282**, 589 (1987).

[10] P. F. Harrison, D. H. Perkins, and W. G. Scott, Phys. Lett. B **458**, 79 (1999).

[11] S. F. King and C. Luhn, Rep. Prog. Phys. **76**, 056201 (2013).

[12] E. Ma, Phys. Rev. D **70**, 031901 (2004).

[13] G. Altarelli and F. Feruglio, Nucl. Phys. **B720**, 64 (2005).

[14] G. Altarelli and F. Feruglio, Nucl. Phys. **B741**, 215 (2006).

[15] K. S. Babu, E. Ma, and J. W. F. Valle, Phys. Lett. B **552**, 207 (2003); B. Adhikary, B. Brahmachari, A. Ghosal, E. Ma, and M. K. Parida, Phys. Lett. B **638**, 345 (2006); M. Honda and M. Tanimoto, Prog. Theor. Phys. **119**, 583 (2008).

[16] B. Brahmachari, S. Choubey, and M. Mitra, Phys. Rev. D **77**, 073008 (2008); **77**, 119901(E) (2008).

[17] Y. Lin, Nucl. Phys. **B813**, 91 (2009); S. F. King, Phys. Lett. B **675**, 347 (2009); G. C. Branco, R. Gonzalez Felipe, M. N. Rebelo, and H. Serodio, Phys. Rev. D **79**, 093008 (2009); Y. Lin, Nucl. Phys. **B824**, 95 (2010); D. Aristizabal Sierra, F. Bazzocchi, I. de Medeiros Varzielas, L. Merlo, and S. Morisi, Nucl. Phys. **B827**, 34 (2010); S. Morisi and E. Peinado, Phys. Rev. D **80**, 113011 (2009); Y. H. Ahn and C.-S. Chen, Phys. Rev. D **81**, 105013 (2010); J. Barry and W. Rodejohann, Phys. Rev. D **81**, 093002 (2010); **81**, 119901(E) (2010); Y. H. Ahn, arXiv:1006.2953; I. de Medeiros Varzielas and L. Merlo, J. High Energy Phys. 02 (2011) 062; Y. H. Ahn, H.-Y. Cheng, and S. Oh, Phys. Rev. D **83**, 076012 (2011).

[18] Y. Shimizu, M. Tanimoto, and A. Watanabe, Prog. Theor. Phys. **126**, 81 (2011).

[19] E. Ma and D. Wegman, Phys. Rev. Lett. **107**, 061803 (2011).

[20] S. F. King and C. Luhn, J. High Energy Phys. 09 (2011) 042.

[21] Y. H. Ahn, H.-Y. Cheng, and S. Oh, Phys. Rev. D **84**, 113007 (2011); S. Antusch, S. F. King, C. Luhn, and M. Spinrath, Nucl. Phys. **B856**, 328 (2012); G.-J. Ding and D. Meloni, Nucl. Phys. **B855**, 21 (2012); S. F. King and C. Luhn, J. High Energy Phys. 03 (2012) 036; Y. H. Ahn and H. Okada, Phys. Rev. D **85**, 073010 (2012); G. C. Branco, R. Gonzalez Felipe, F. R. Joaquim, and H. Serodio, Phys. Rev. D **86**, 076008 (2012); Y. H. Ahn and S. K. Kang, Phys. Rev. D **86**, 093003 (2012); H. Ishimori and E. Ma, Phys. Rev. D **86**, 045030 (2012).

[22] G. Altarelli, F. Feruglio, L. Merlo, and E. Stamou, J. High Energy Phys. 08 (2012) 021.

[23] G. Altarelli, F. Feruglio, and L. Merlo, Fortschr. Phys. **61**, 507 (2013); E. Ma, A. Natale, and A. Rashed, Int. J. Mod. Phys. A **27**, 1250134 (2012); Y. H. Ahn, S. Baek, and P. Gondolo, Phys. Rev. D **86**, 053004 (2012); Y. BenTov, X.-G. He, and A. Zee, J. High Energy Phys. 2012, 093 (2012); E. Ma, Phys. Rev. D **86**, 117301 (2012); M.-C. Chen, J. Huang, J.-M. O'Bryan, A. M. Wijangco, and F. Yu, J. High Energy Phys. 02 (2013) 021; M. Holthausen, M. Lindner, and M. A. Schmidt, Phys. Rev. D **87**, 033006 (2013); I. de Medeiros Varzielas and D. Pidt, J. High Energy Phys. 03 (2013) 065; N. Memenga, W. Rodejohann, and H. Zhang, Phys. Rev. D **87**, 053021 (2013); S. Antusch, S. F. King, and M. Spinrath, Phys. Rev. D **87**, 096018 (2013); S. F. King, S. Morisi, E. Peinado, and J. W. F. Valle, Phys. Lett. B **724**, 68 (2013); A. Kadosh, J. High Energy Phys. 06 (2013) 114; M. Borah, B. Sharma, and M. K. Das, Nucl. Phys. **B885**, 76 (2014); Y. H. Ahn, S. K. Kang, and C. S. Kim, Phys. Rev. D **87**, 113012 (2013); S. F. King, Phys. Lett. B **724**, 92 (2013); S. Antusch, C. Gross, V. Maurer, and C. Sluka, Nucl. Phys. **B877**, 772 (2013); S. Morisi, D. V. Forero, J. C. Romo, and J. W. F. Valle, Phys. Rev. D **88**, 036001 (2013); P. M. Ferreira, L. Lavoura, and P. O. Ludl, Phys. Lett. B **726**, 767 (2013); S. Antusch and D. Nolde, J. Cosmol. Astropart. Phys. 10 (2013) 028; S. Antusch, C. Gross, V. Maurer, and C. Sluka, Nucl. Phys. **B879**, 19 (2014); Y. H. Ahn and S. Baek, Phys. Rev. D **88**, 036017 (2013); D. Borah, Nucl. Phys. **B876**, 575 (2013); G.-J. Ding, S. F. King, and A. J. Stuart, J. High Energy Phys. 12 (2013) 006; A. E. Carcamo Hernandez, I. de Medeiros Varzielas, S. G. Kovalenko, H. Pas, and I. Schmidt, Phys. Rev. D **88**, 076014 (2013); Y. Zhao and P.-F. Zhang, arXiv:1402.5834; Y. Grossman and W. H. Ng, arXiv:1404.1413; D. A. Sierra and I. de Medeiros Varzielas, J. High Energy Phys. 07 (2014) 042; V. V. Vien and H. N. Long, arXiv:1405.4665.

[24] For a review, see S. Davidson, E. Nardi, and Y. Nir, Phys. Rep. **466**, 105 (2008), and references therein.

[25] E. E. Jenkins and A. V. Manohar, Phys. Lett. B **668**, 210 (2008).

[26] I. K. Cooper, S. F. King, and C. Luhn, Nucl. Phys. **B859**, 159 (2012).

[27] C. Hagedorn, E. Molinaro, and S. T. Petcov, J. High Energy Phys. 09 (2009) 115.

[28] S. Pascoli, S. T. Petcov, and A. Riotto, Phys. Rev. D **75**, 083511 (2007).

[29] S. Blanchet, P. Di Bari, and G. G. Raffelt, J. Cosmol. Astropart. Phys. 03 (2007) 012.

[30] S. Davidson, J. Garayoa, F. Palorini, and N. Rius, J. High Energy Phys. 09 (2008) 053.

[31] C. D. Froggatt and H. B. Nielsen, Nucl. Phys. **B147**, 277 (1979).

[32] G. Altarelli and F. Feruglio, Rev. Mod. Phys. **82**, 2701 (2010).

[33] B. Adhikary and A. Ghosal, Phys. Rev. D **78**, 073007 (2008); S.-F. Ge, H.-J. He, and F.-R. Yin, J. Cosmol. Astropart. Phys. 05 (2010) 017.
[34] G. Altarelli and D. Meloni, J. Phys. G **36**, 085005 (2009).
[35] J. Barry and W. Rodejohann, Nucl. Phys. **B842**, 33 (2011); S. F. King, A. Merle, and A. J. Stuart, J. High Energy Phys. 12 (2013) 005.
[36] S.-F. Ge, D. A. Dicus, and W. W. Repko, Phys. Lett. B **702**, 220 (2011); Phys. Rev. Lett. **108**, 041801 (2012); D. Hernandez and A. Y. Smirnov, Phys. Rev. D **86**, 053014 (2012).
[37] P. A. R. Ade *et al.* (Planck Collaboration), Astron. Astrophys. **571**, A16 (2014).
[38] S. M. Bilenky and C. Giunti, Mod. Phys. Lett. A **27**, 1230015 (2012).
[39] Y. Huang and B.-Q. Ma, arXiv:1407.4357.
[40] M. Fukugita and T. Yanagida, Phys. Lett. B **174**, 45 (1986).
[41] M. Flanz, E. A. Paschos, and U. Sarkar, Phys. Lett. B **345**, 248 (1995); **382**, 447(E) (1996).
[42] L. Covi, E. Roulet, and F. Vissani, Phys. Lett. B **384**, 169 (1996).
[43] M. Plumacher, Z. Phys. C **74**, 549 (1997).
[44] W. Buchmuller and M. Plumacher, Phys. Lett. B **431**, 354 (1998).
[45] W. Buchmuller, P. Di Bari, and M. Plumacher, Ann. Phys. **315**, 305 (2005).
[46] G. F. Giudice, A. Notari, M. Raidal, A. Riotto, and A. Strumia, Nucl. Phys. **B685**, 89 (2004).
[47] J. A. Harvey and M. S. Turner, Phys. Rev. D **42**, 3344 (1990).
[48] G. Engelhard, Y. Grossman, and Y. Nir, J. High Energy Phys. 07 (2007) 029.
[49] G. Engelhard, Y. Grossman, E. Nardi, and Y. Nir, Phys. Rev. Lett. **99**, 081802 (2007).
[50] S. T. Petcov, S. Profumo, Y. Takanishi, and C. E. Yaguna, Nucl. Phys. **B676**, 453 (2004).
[51] S. T. Petcov, W. Rodejohann, T. Shindou, and Y. Takanishi, Nucl. Phys. **B739**, 208 (2006).
[52] A. Djouadi and J. Quevillon, J. High Energy Phys. 10 (2013) 028.
[53] C. L. Bennett *et al.* (WMAP Collaboration), Astrophys. J. Suppl. Ser. **208**, 20 (2013).
[54] A. Pilaftsis, Phys. Rev. D **56**, 5431 (1997); A. Pilaftsis and T. E. J. Underwood, Nucl. Phys. **B692**, 303 (2004).